ISSN 1063-7826, Semiconductors, 2012, Vol. 46, No. 2, pp. 188–192. © Pleiades Publishing, Ltd., 2012.
Original Russian Text © Yu.Yu. Bacherikov, N.E. Korsunska, V.P. Kladko, E.F. Venger, N.P. Baran, A.V. Kuchuk, A.G. Zhuk, 2012, published in Fizika i Tekhnika Poluprovodnikov, 2012, Vol. 46, No. 2, pp. 198–203.

MICROCRYSTALLINE, NANOCRYSTALLINE, POROUS, AND COMPOSITE SEMICONDUCTORS

Structural Transformations in ZnS:Cu in the Course of Thermal Annealing

Yu. Yu. Bacherikov^, N. E. Korsunska, V. P. Kladko, E. F. Venger, N. P. Baran, A. V. Kuchuk, and A. G. Zhuk

Lashkaryov Institute of Semiconductor Physics, National Academy of Sciences of Ukraine, pr. Nauki 45, Kiev, 03028 Ukraine

^e-mail: yuyu@isp.kiev.ua

Submitted July 5, 2011; accepted for publication July 11, 2011

Abstract—The influence of annealing at 800°C on the photoluminescence, electron spin resonance, and X-ray diffraction spectra of powder-like ZnS:Cu, obtained by the self-propagating high-temperature synthesis of a charge, consisting of Zn, S, and CuCl, is studied. It is shown that variation in the material's heating rate up to the annealing temperature leads to a nonmonotonic variation in the spectral location and full-width at half-maximum of the photoluminescence band in the blue-green spectral region, as well as in the Mn^{2+} paramagnetic center concentration. It is established that the cubic and hexagonal ZnS phases, as well as the ZnO and CuZn phases, are present in the powder after synthesis. It is shown that annealing of the obtained powder at 800°C leads to three processes: the transformation of the hexagonal ZnS phase into the cubic phase, the oxidation of ZnS and CuZn, and the diffusion of Cu into the bulk of the ZnS microcrystals from the CuZn phase. A model attributing the observed variations in luminescence and electron spin resonance spectra to the diffusion of Cu and Mn impurities into the microcrystal bulk, particularly from the CuZn phase, and to their accumulation at extended defects is suggested.

DOI: 10.1134/S1063782612020030

1. INTRODUCTION

Currently, ZnS-based phosphors are widely used as they are most efficient in the blue-green spectral region. This is associated with the relatively low cost of their fabrication and the simplicity of standard technologies for their synthesis [1, 2]. To attain luminescence in this spectral region, Cu doping of ZnS is usually used, which leads to the emergence of two bands, namely, a blue band with a peak at 440–465 nm and a green band with a peak at 505–530 nm, or the so-called *B*-Cu and *G*-Cu bands [3, 4]. However, their manifestation in the photoluminescence (PL) spectra strongly depends on the synthesis conditions and the material's subsequent processing treatments, which affect the formation of luminescence centers. This is associated not only with the dependence of the Cu center concentration ratio, which determine the blue and green PL bands, on synthesis conditions and subsequent treatments, but also with the fact that the self-activated luminescence centers [2–4] and oxygen-induced centers [3–5], whose emissive characteristics also depend on the production parameters, can contribute to luminescence in the blue–green region.

It was shown [6] that it is possible to control the ratio of contributions of Cu luminescence centers, which determine the blue and green PL bands in the ZnS:Cu spectra, by varying the supplied heat flow (the time of furnace heating up to $T = 800$°C) during thermal doping of ZnS from the CuCl charge at a certain annealing temperature and time, as well as cooling time. However, process mechanisms leading to variation in the contributions of blue and green luminescence to the PL spectrum remain unclarified. In particular, when analyzing these results, the ZnS doping process was divided into two stages [6]. The first stage involves processes associated with adsorption of the doping impurity by the base material, and the second stage involves processes associated with impurity diffusion into the material bulk and the formation of blue and green luminescence centers in ZnS:Cu. However, their roles were not established unambiguously.

To clarify these issues, we studied the influence of annealing modes on the luminescent and structural characteristics, as well as on the electron spin resonance (ESR) spectra of powdered ZnS obtained by self-propagating high-temperature synthesis (SHS), doped with Cu during growth.

2. EXPERIMENTAL

The studied ZnS:Cu crystals were synthesized by SHS at temperatures that ensure the interaction of S and Zn [7], and were doped during growth. The ratio of the initial materials was as follows: 0.45 mol Zn, 0.56 mol S, and 0.006 mol CuCl. Subsequent thermal annealing at 800°C was performed in a laboratory quartz furnace. The atmosphere ingress to the annealed powder was restricted by a granulated-coal gas gate. The temperature mode of annealing was monitored using a

thermocouple located in the area of the annealed material. The annealing time was 120 min, and the heating time of the furnace to the annealing temperature t_h varied from 15 to 240 min. The cooling time of the furnace was constant in all cases.

The PL spectra were measured using an SDL-2 installation. The PL was excited by the radiation of a DKSSh-150 xenon lamp through an MDR-12 monochromator with the wavelength $\lambda = 337$ nm.

The ESR spectra were detected using a Varian-12 radiospectrometer operating in a 3-cm wavelength range with high-frequency magnetic field modulation of 100 kHz. When studying the ESR spectra, we used samples that contain identical amounts of powdered ZnS:Cu.

X-ray diffraction was studied using a Philips X'Pert-MRD X-ray diffractometer (CuK_α radiation, wavelength $\lambda = 0.15418$ nm) in the Bragg–Brentano geometry.

All measurements were performed at room temperature.

3. RESULTS AND DISCUSSION

Figure 1 shows the PL spectra of the samples under study for various heating times of the furnace to the annealing temperature. It is seen from Fig. 1 that the PL spectra are shaped as a broad band in the blue–green region, the location of whose peak (λ_{max}) and full width at half-maximum (FWHM) depend on t_h. The corresponding dependences are presented in the inset in Fig. 1. We note that point 0 of the abscissa corresponds to the unannealed sample. It is seen from Fig. 1 that the peak location shifts initially to longer wavelengths and then to shorter wavelength as t_h increases. In this case, FWHM initially decreases and then increases. Such behavior of the observed band's spectral characteristics means that it is nonelementary. A decrease in the width with a simultaneous shift of the peak to longer wavelengths indicates a decrease in the contribution of luminescence centers determining the band in the blue spectral region, while a subsequent increase with a shift of the peak to shorter wavelengths indicates an increase in their contribution.

It was already noted that the observed band can be caused by Cu luminescent centers [2–4, 8–10], as well as by centers of oxygen [3, 4, 8–10] and self-activated emission [2, 4, 8, 9]. To reveal the causes of the shift of the peak in the observed PL band, let us compare our results with the data [6], where the blue and green bands induced by the Cu impurity were well distinguished. It was shown in [6] that the contribution of the blue band initially decreases and then increases as t_h increases. This agrees with the change in the peak location and in the width of the observed band. Therefore, we may assume that a variation in the intensity ratio of, particularly, the blue and green Cu bands also occurs in our case, which leads to the peak shift in the PL band.

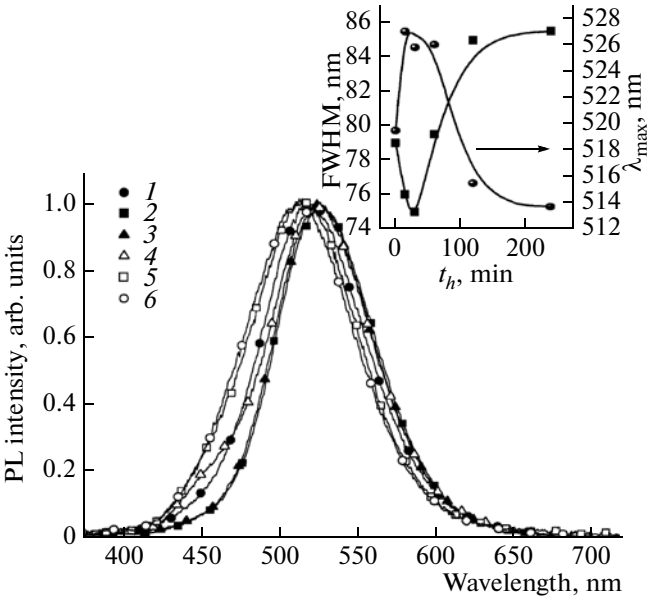

Fig. 1. Normalized-to-maximum photoluminescence (PL) spectra of the ZnS:Cu samples (*1*) unannealed and (*2–5*) annealed at $T = 800$°C for 120 min. Furnace heating times to the annealing temperature were (*2*) 15, (*3*) 30, (*4*) 60, (*5*) 120, and (*6*) 240 min. Dependences of the peak wavelength λ_{max} and the band width FWHM on the furnace heating time to the annealing temperature are in the inset (point 0 in the abscissa corresponds to the unannealed sample).

We note that, to date, the nature of luminescent centers determining blue and green Cu bands in ZnS is studied in detail in many respects [3, 4, 8–12]. It was shown that the centers responsible for the emergence of the *G*-Cu band are isolated Cu ions that substitute Zn ions in the ZnS lattice [3, 8–10]. It is established that the symmetry of such a center is no lower than the symmetry of a regular site of the cubic or hexagonal ZnS lattice. Consequently, the coactivator is not included in the center composition. The *B* band is attributed [2, 8–13] to the formation of associates of the close donor–acceptor pair type Cu_i–Cu_{Zn} [2, 8, 13] or Cu_{Zn}–Cu_{Zn} [9–12].

The ESR spectrum of the samples under study is shown in Fig. 2a. The six clearly pronounced lines are characteristic of paramagnetic Mn^{2+} centers (Mn_{Zn}) in disordered systems with a low Mn concentration. The observed spectrum is described by the following parameters: the spectroscopic splitting factor $g = 2.0026$, the hyperfine interaction constant $A = 6.69$ mT, and the line half-width is 0.12–0.13 mT. The obtained parameters are characteristic of Mn^{2+} ions in a cubic modification of ZnS [14]. We note that the Mn impurity was not specially introduced into the ZnS:Cu phosphor. It seems likely that it is an accompanying impurity of the Zn or CuCl initial components used in the course of synthesis.

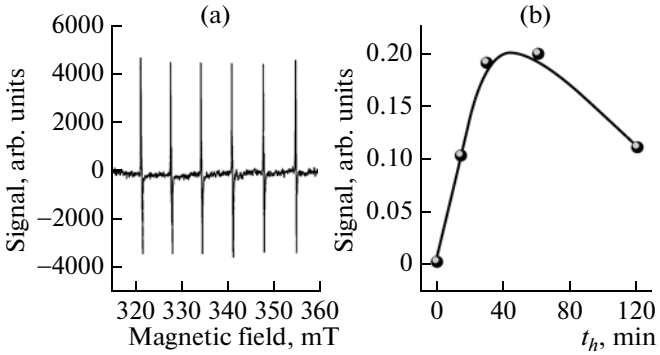

Fig. 2. (a) ESR spectrum of Mn^{2+} ions in the ZnS:Cu sample and (b) dependence of the ESR signal intensity of Mn^{2+} ions on the furnace heating time to the annealing temperature. (b): point 0 in the abscissa corresponds to the unannealed sample.

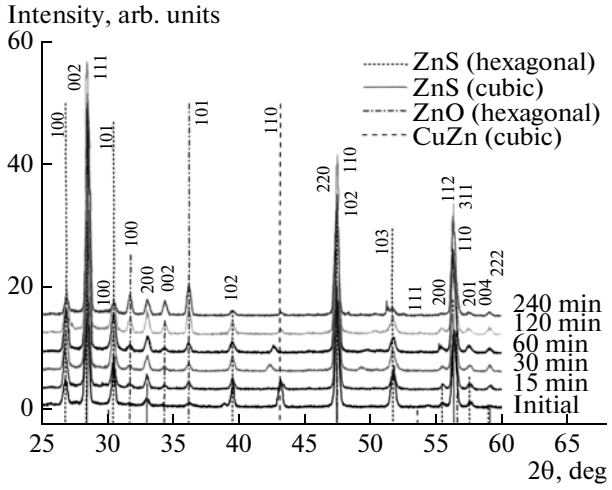

Fig. 3. X-ray diffraction spectra of powdered ZnS:Cu samples before and after annealing at $T = 800°C$ for the furnace heating time to the annealing temperature in the range 15 to 240 min.

The general shape of the ESR spectrum was unvaried after annealing and independent of t_h. However, it turned out that the ESR signal intensity, determined by the difference between maximum and minimum of differential spectrum, substantially increases during annealing. For all applied furnace heating times, the ESR signal intensity after annealing was substantially higher than for the initial sample (Fig. 2b). In addition, the intensity of this signal, i.e., the Mn^{2+} ion concentration, depends on t_h (Fig. 2b); as t_h increases, the concentration of these ions initially increases and then decreases. The highest concentration of Mn^{2+} ions in the phosphor is observed for the same t_h, at which we observed the maximal contribution of the Cu_{Zn} centers determining the green band to the PL spectra.

Analysis of the presented PL and ESR results indicates substantial variations in the system of local powdered ZnS:Cu centers with variation of the heating rate up to the annealing temperature of 800°C. To reveal the causes of these variations, we studied the phase composition of powdered ZnS:Cu using X-ray diffraction. The results of these studies are presented in Fig. 3.

It is seen from Fig. 3 that the initial powder consists of the cubic (zinc blende) and hexagonal (wurtzite) ZnS phases. The intense (111) reflection of the cubic ZnS phase indicates that it is dominant in our samples. In addition, a small amount of the hexagonal ZnO phase and CuZn compounds with a cubic lattice (peak at the angle $2\theta \approx 43°$) are present in the initial powder. Formation of the CuZn alloy may be caused by violation of the ZnS stoichiometry during synthesis and by the emergence of excess Zn, as well as by the decomposition of CuCl, which leads to the formation of free Cu.

Annealing leads to variation in the powder's phase composition, and these variations depend on the time of sample heating to the annealing temperature. The ratio of the intensity of the ZnS hexagonal phase (100) reflection to the intensity of the ZnS cubic phase (200) reflection is shown in Fig. 4a. It is seen from Fig. 4a that this ratio decreases as t_h increases, which indicates a decrease in the fraction of the hexagonal phase in the ZnS:Cu grains.

A gradual increase in the intensity of ZnO phase reflections is also observed with an increase in t_h. This is seen in Fig. 4c, where we represent the t_h-dependences of the intensity ratios of the ZnO (101) reflection to the ZnS hexagonal phase (100) reflection and the ZnS cubic phase (200) reflection. It is seen from Fig. 4c that the contribution of ZnO is insignificant at small t_h, but as t_h increases, oxidation becomes more intense.

In addition to the described phase transformations, structural transformations of CuZn also occur during annealing. As t_h increases, the peak attributed to the CuZn phase shifts initially to lower angles (at $t_h = 15$ and 30 min), and then to the opposite side (Fig. 4d). Its intensity gradually decreases. The peak shift is apparently caused by a change in the composition of the CuZn alloy, and the shift towards lower angles corresponds to a decrease in the Cu content. Such a shift with a simultaneous decrease in the peak intensity indicates the diffusion of Cu into the microcrystal bulk. This means that the Cu atoms are nonuniformly distributed in the microcrystal bulk after synthesis. We note that the CuS phase, which is assumed to participate in Cu doping, was not observed in our case [15].

The peak shift towards higher angles, caused by CuZn, corresponds to a decrease in the alloy's Zn content. This can be attributed to the oxidation of Zn, which is consistent with an increase in the content of the ZnO phase in the powder (Fig. 4c). This process

should also lead to a decrease in the intensity of the CuZn peak.

Variation in the phase composition of the powdered ZnS with an increase in the heating time leads to a variation in the size of the cubic and hexagonal phases' coherent scattering region (D). The dependence of the value D, estimated using the Scherrer formula, on the furnace heating time to the annealing temperature for both phases is shown in Fig. 4b. It is seen in Fig. 4b that D for the cubic phase initially increases as t_h increases and then decreases. However, for the hexagonal phase, D continuously decreases. It is evident that a change in D can be caused by both the transformation of the hexagonal phase into the cubic and by the oxidation of ZnS. In this case, the character of the dependence $D(t_h)$ is determined by the contribution of these two processes. Therefore, it is natural to attribute an increase in D for the cubic phase, which is observed at small t_h when the role of oxidation is not very significant, to the transformation of the hexagonal phase into the cubic, while a decrease in D with an increase in t_h can be attributed to the dominant contribution of oxidation. It is evident that for the hexagonal phase, both these processes should lead to a decrease in D, which is observed experimentally.

Thus, in addition to the transformation of the hexagonal phase into the cubic, two processes occur during the annealing of powdered ZnS:Cu. These are the doping of microcrystals with Cu from the CuZn alloy and oxidation caused by the presence of oxygen in the atmosphere, in which the samples were annealed. It should be noted that the size of the coherent scattering region for both ZnS phases, ~(15–30) nm, is substantially smaller than the grain size for ZnS, ~(2–6) μm, which was estimated using scanning electron microscopy. Consequently, numerous interphase boundaries are present inside the grains. Correspondingly, the observed oxidation of both ZnS phases implies the diffusion of oxygen along the interphase boundaries. This fact agrees with the notion that these boundaries are places of rapid impurity diffusion. It is possible that the CuZn phase is also present at these boundaries, i.e., inside the ZnS grains, although it seems more probable that it is located on their surface.

Based on the data of X-ray studies, we may suggest the following model for interpreting the nonmonotonicity of the PL band peak shift and the variation in the Mn^{2+} ion concentration during annealing.

Copper is distributed nonuniformly during ZnS synthesis, therefore, both isolated Cu_{Zn} atoms, which are the centers of green luminescence, and the complexes that cause the blue band, which are arranged in places of Cu accumulation, are present in the initial samples. The latter are apparently present near the CuZn phase. During annealing, microcrystals are additionally doped with Cu from this phase. Initially (at small t_h), Cu is incorporated into Zn sites forming centers of green luminescence. This leads to an

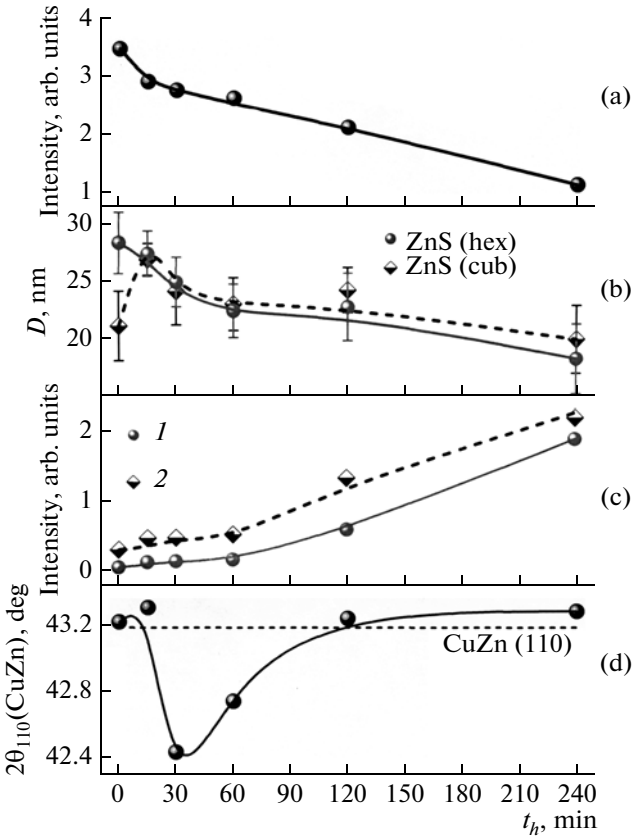

Fig. 4. The t_h dependences of (a) the intensity ratio of the (100) reflection for the hexagonal ZnS (hex) phase to the (200) reflection for the cubic ZnS (cub) phase; (b) the size of coherent scattering regions ZnS (hex) and ZnS (cub); (c) the intensity ratio of the (101) reflection for ZnO to the ZnS hexagonal (hex) phase (100) and ZnS cubic (cub) phase (200) reflections, (*1*) and (*2*), respectively; and (d) the location of the (110) peak of the CuZn alloy diffraction curve $2\theta_{110}$ (CuZn).

increase in the contribution of the green band to the PL spectrum and, correspondingly, to a shift of the PL peak to longer wavelengths. As t_h increases, the amount of Cu incorporated into the microcrystals increases, which promotes the formation of complexes determining the blue band and causes a shift of the PL band to shorter wavelengths.

Similar processes, it seems, also take place with Mn atoms. Indeed, annealing leads to a substantial increase in the ESR signal intensity, which indicates the emergence of isolated Mn_{Zn} atoms in the microcrystal bulk. Their source may be the Mn atom clusters or, for example, the CuZn alloy, which can contain Mn as a background impurity. As t_h increases, the amount of Mn incorporated into the ZnS increases, which leads to an increase in the ESR signal amplitude at t_h = 15–16 min. A further decrease in the signal amplitude is apparently caused by the accumulation of Mn at extended defects. In this case, the signal from the Mn^{2+} ions decreases since the formation of clusters

leads to the disappearance of isolated Mn lines and to the emergence of a wide (20–30 mT) line with a substantially smaller amplitude [16]. However, we had not observed this line experimentally, it seems, due to an insufficiently high cluster concentration. We note that the accumulation at extended defects can also take place for Cu atoms, which also promotes the emergence of blue luminescence centers.

It should be noted that the shift of the PL band peak to longer wavelengths can be, in principle, attributed not only to an increase in the contribution of the ZnS *G* band but also to the formation of the ZnO phase, since the presence of green luminescence is also characteristic of it. However, the shift would continuously increase with an increase in t_h in this case.

4. CONCLUSIONS

As a result of studying the influence of annealing on the PL, ESR, and X-ray diffraction spectra of powdered ZnS:Cu samples obtained by self-propagating high-temperature synthesis, it is shown that variation in the heating rate of the material up to the annealing temperature can be controlled by the concentration ratio of centers that give rise to the blue and green luminescence bands associated with the Cu impurity, as well as by the concentration of the Mn^{2+} paramagnetic centers. As the heating time increases, the contribution of centers that govern the green band initially increases and then decreases. The concentration of Mn^{2+} centers varies similarly. It is established that annealing at 800°C transforms the hexagonal ZnS phase into the cubic, increases the ZnO content, and leads to a nonmonotonic variation in the composition of the CuZn alloy. As the heating time increases, the Cu content in the alloy initially decreases and then increases. A decrease in the Cu content can be attributed to the fact that its diffusion into the ZnS microcrystal bulk is dominant, while an increase in the Cu content can be attributed to the oxidation of Zn. Cu-doping of microcrystals and an increase in the concentration of Mn^{2+} centers after annealing indicates that the Cu and Mn atoms are located nonuniformly in the bulk after synthesis. We suggested a model for interpreting the observed variations in the luminescence and electron spin resonance spectra in terms of microcrystal doping with Cu and Mn and accumulation of these impurities at extended defects.

REFERENCES

1. O. N. Kazankin, L. Ya. Markovskii, I. A. Mironov, F. M. Pekerman, and L. N. Petoshina, *Inorganic Luminophors* (Khimiya, Leningrad, 1975) [in Russian].
2. A. M. Gurvich, *Introduction to the Physical Chemistry of Crystal Phosphors* (Vyssh. Shkola, Moscow, 1971) [in Russian].
3. N. K. Morozova, D. A. Mideros, V. G. Galstyan, and E. M. Gavrishchuk, Semiconductors **42**, 1023 (2008).
4. L. A. Gromov and V. A. Trofimov, Zh. Fiz. Khim. **55**, 2629 (1981).
5. N. K. Morozova and V. A. Kuznetsov, *Zinc Sulfide: Preparation and Optical Properties* (Nauka, Moscow, 1987) [in Russian].
6. Yu. Yu. Bacherikov, I. S. Golovina, and N. V. Kitsyuk, Phys. Solid State **48**, 1872 (2006).
7. S. V. Kozytckyy, V. P. Pysarskyy, and D. D. Polishchuk, Phys. Chem. Solid State **4**, 749 (2003).
8. M. Aven and J. S. Prener, *Physics and Chemistry of II–VI Compounds* (North-Holland, Amsterdam, New York, 1967; Mir, Moscow, 1970).
9. U. Kh. Nymm, Dep. VINITI, No. 4219-80 (1980).
10. G. E. Arkhangel'skii, N. N. Grigor'ev, A. V. Lavrov, and M. V. Fok, Tr. FIAN **164**, 103 (1985); M. A. Rizakhanov, M. M. Khamidov, and I. Ya. Abramov, Sov. Phys. Semicond. **12**, 1301 (1978).
11. N. A. Vlasenko and E. N. Pavlova, Opt. Spektrosk. **12**, 550 (1962).
12. Z. P. Ilyukhina, E. P. Panasyuk, V. F. Tunitskaya, and T. F. Filina, Tr. FIAN SSSR **59** (38) (1972).
13. M. M. Sychev, E. V. Komarov, L. V. Grigor'ev, S. V. Myakin, I. V. Vasil'eva, A. I. Kuznetsov, and V. P. Usacheva, Semiconductors **40**, 1016 (2006).
14. M. V. Vlasova, N. G. Kakazei, A. M. Kalinchenko, and A. S. Litovchenko, *Radiospectroscopic Properties of Inorganic Materials. A Handbook* (Nauk. Dumka, Kiev, 1987) [in Russian].
15. A. A. Bundel', A. V. Vishnyakov, Z. I. Guretskaya, S. S. Galaktionov, V. N. Zubkovskaya, L. A. Smorodinova, Ya. L. Kharif, Yu. M. Khozhainov, V. A. Chashchin, and A. T. Yagodina, Izv. AN SSSR, Ser. Fiz. **35**, 1461 (1971).
16. T. H. Yeom, Y. H. Lee, T. S. Hahn, M. H. Oh, and S. H. Choh, J. Appl. Phys. **79**, 1004 (1996).

Translated by N. Korovin